Phenomenology of the Pokaran PNE experiment

R CHIDAMBARAM, S K SIKKA and SATISH C GUPTA

Physics Group, Bhabha Atomic Research Centre, Trombay, Bombay 400 085, India

Abstract. The phenomenology of the Pokaran PNE experiment (yield – 12 kiloton of TNT) conducted in a shale-sandstone rock, 107 meters underground, is described with the aid of computations using a one-dimensional spherical symmetric rock mechanics computer code developed by the authors. The calculated values of cavity radius, spall velocity and extent of rock fracturing are in good agreement with the observed values. The principal mechanism for crater formation at Pokaran was spall and the relatively smaller crater dimensions and non-venting of radioactivity gases were due to lower kinetic energy transferred to the shale-sandstone rock.

Keywords. Pokaran; peaceful nuclear explosions; crater; non-venting.

PACS No. 91·90; 91·60.

1. Introduction

India's first and only peaceful nuclear explosion experiment was carried out in Rajasthan desert on 18 May 1974 at a place near Pokaran. The object of the experiment was to study the explosion phenomenology, fracturing effects in rocks, ground motion, containment of radioactivity and postshot access of the region around the point of detonation (Chidambaram and Ramanna 1975). Such studies are important in the context of possible applications of peaceful nuclear explosions (PNES).

A plutonium device, of yield 12 kt equivalent of TNT,* was emplaced in a shale medium, at a depth of 107 m, in a chamber at the end of an L-shaped hole. Upon detonation, the ground surface above the emplacement point rose with a velocity of about 25–30 m/sec to form a dome 170 m in diameter and 34 m in height. The mound remained intact during its growth and fall and no venting of radioactive gases was observed. The resultant apparent crater, measured with respect to the preshot ground surface, has an average radius of 47 m and depth of 10 m.

The phenomenology of the event is interesting as it is the only recorded case of an explosion which produced a crater, although a very shallow one, and yet was completely contained from the radioactivity point of view. Also, a comparison of the Pokaran crater dimensions with other cratering experiments in hard rock (figures 1 and 2) shows that the Pokaran crater was smaller. At its scaled depth of burial (SDOB) $51·5 \, \text{m/kt}^{1/3·4}$, the scaled radius and depth for a hard rock cratering experiment are predicted to be (Nordyke 1970) $SR_a = 27 \, \text{m/kt}^{1/3·4}$ and $SD_a = 14 \, \text{m/kt}^{1/3·4}$, compared to the values of $23 \, \text{m/kt}^{1/3·4}$ and $5 \, \text{m/kt}^{1/3·4}$ respectively observed for the Pokaran experiment. The

---

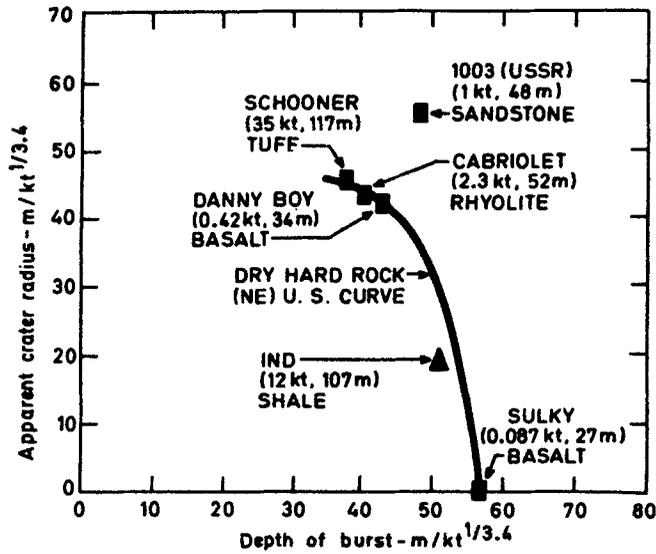* $1 \, \text{kt} = 4·186 \times 10^9$ ergs, the explosive energy equivalent of 1000 tonnes of TNT.

Figure 1. Scaled apparent crater radius versus the scaled depth of burst for nuclear cratering explosions in hard rock.
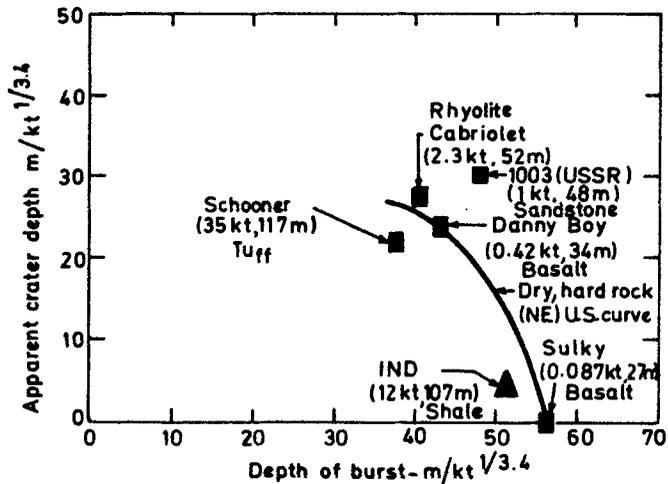

Figure 2. Scaled apparent crater depth versus the scaled depth of burst for nuclear cratering explosions in hard rock.

peak vertical velocity of 25 to 30 m/sec for the latter also is lower than the value ~ 40 m/sec, as read from figure 6 of Toman (1970). In this paper, we have tried to explain these observations based on computer calculations using 'OCENER', a one-dimensional spherical rock mechanics code developed in our laboratory (Gupta *et al* 1979a; Gupta 1979).

2. One-dimensional rock mechanics code

The computer code developed by us has many similarities with the American code 'soc' (Cherry 1967; Cherry and Petersen 1970; Schatz 1973) and the French code 'S' (Michaud and Maury 1970). Some of the physical-mechanical processes associated with the propagation of the stress field set up in a geological medium by a sudden release of the explosive energy of a nuclear device (Teller *et al* 1968) are vaporisation, melting, crushing, fracture and motion of the rock. Also the stress wave gets reflected at the free ground surface and this transfers additional kinetic energy to the rock medium. The final crater dimensions depend upon the total kinetic energy transferred to the region above the explosion-produced cavity. Our code models these events in one dimension, in spherical symmetry, by finite difference solutions of the laws of mass, momentum and energy conservation, and employs the physical and mechanical properties of the rock material under different stress conditions.

In a given calculation, the medium surrounding the explosion point is divided into spherical meshes and the conservation laws are expressed in a Lagrangian co-ordinate system, so that the conservation of mass is automatically achieved. From the initial stress field at time t, the momentum equation (equation of motion) is solved to ascertain the acceleration of each zone boundary. Accelerations, when allowed to act over a small time increment Δt, produce new velocities and subsequently new displacements of the zone boundaries. These displacements produce strains which, depending upon the equation of state of the rock, produce the new stress field. The cycle is repeated after each time increment Δt. The steep shock fronts are handled in the program by the artificial viscosity method due to von Neumann and Richtmayer (1950). Some of the outputs of this program are the following:

(i) the amount of shock-vapourised rock,

(ii) the amount of shock-melted rock,

(iii) the radius of the cavity and the pressure inside it at any given time,

(iv) profiles of shock position versus time, peak stress (both hydrostatic and deviatoric) versus radius, particle velocity versus radius, etc.,

(v) spall velocities of the mesh points as the reflected tensile wave from the surface travels towards the growing cavity,

(vi) kinetic energy transferred to the medium, and

(vii) the extent and type of rock failure (ductile or fracture).

More details of the code are given elsewhere (Gupta *et al* 1979a).

3. Medium properties*

The geology around the emplacement point has been briefly described by Chidambaram and Ramanna (1975). The shot point was located in a sedimentary

---

* The measurements of the various medium properties reported in this section were carried out in several divisions of BARC and elsewhere.
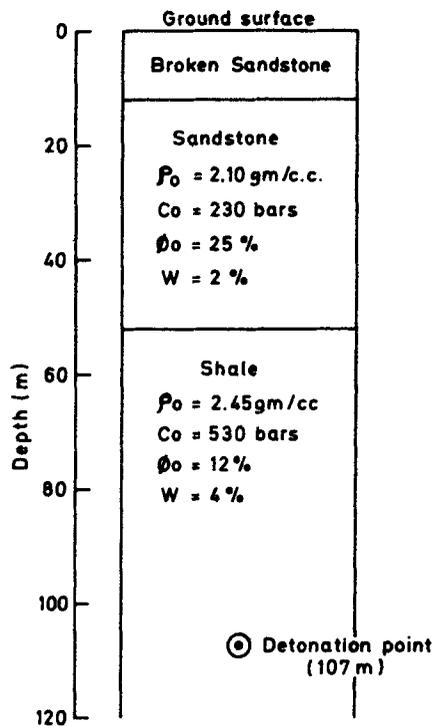
Figure 3. Vertical geologic section adopted for calculations.

formation and the area surrounding the surface ground zero was a flat terrain covered with sand and sandy loam type of soil. The section of the geological structure adopted for the calculations is shown in figure 3. Some of the measured physical and mechanical properties are also shown. The chemical composition of the rocks suggests that the major constituent of these rocks is SiO_2 and the rock can be classified as 'sedimentary SiO_2 rock type'.

3.1 *P-V curves*

The experimental shock Hugoniot data for Pokaran shale* are plotted in figure 4 along with data for several shales and sandstones[†] found in USA. It can be seen that an 'average' curve for a shale medium can be drawn independent of initial density and hence of porosity. This implies that the compressibility at higher pressures does not vary much with minor variations of the rock constituents and is a function of grain density only. This appears to be reasonable since with increasing pressure, the pore collapse and porosity disappears irreversibly at about 40 kbar (Stephens *et al* 1969). Such averaging of the Hugoniot data for calculations for parameters studies using computer codes has also been done by Hearst (1971) for alluvium and by Butkovich (1973) for granite, basalt and tuff rocks. It is interesting to note that the Hugoniot curve calculated for Pokaran shale ($\rho = 2.45$ g/cm^3) using the Butkovich's (1973) prescription, matches well with the 'average' curve. The P-V curve for Pokaran shale, therefore,

---

* The sample for these measurements had density of 2·22 g/cm^3.

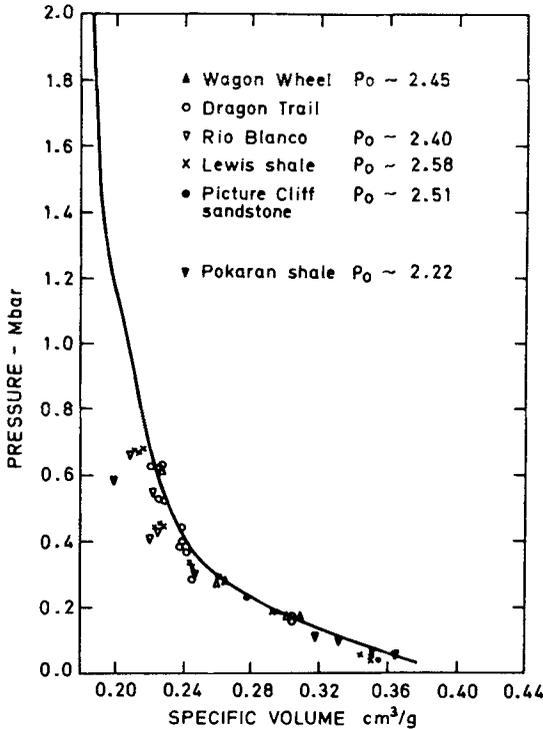[†] These data for other rocks are taken from figure 2 of Terhune (1973).

Figure 4. Shock Hugoniot for Pokaran shale compared with various sandstones and shales. Full curve is the one calculated for $\rho_0 = 2\cdot45$ g/cm^3 using PMUGEN.

was calculated, including the lower pressure range (below 40 kbar), employing a Trombay program PMUGEN based on Butkovich's prescription (Gupta 1979). For Pokaran sandstone, since the shock wave decays to less than 5 kbar when it reaches shale-sandstone interface, the P-V curve is required only in the low pressure regime. This also is calculated using the program PMUGEN.

3.2 *Strength curves*

Since the facilities to carry out triaxial tests on rock samples were not available, the measured values of unconfined compressive strength of the rock have been used to estimate the strength curves employing the expression given by Gupta and Sikka (1978).

$$C/C_0 = 1 + k(\sigma_3/C_0)^n, \tag{1}$$

where C is the confined compressive strength at the confining pressure of σ_3 and C_0 is the unconfined compressive strength ($\sigma_3 = 0$). k and n are constants for a given rock type. The values $k = 2\cdot1$ and $n = 0\cdot64$ for shales and $k = 3\cdot2$ and $n = 0\cdot67$ for sandstones were employed. The brittle ductile points are placed at

$$J_m = 0\cdot8P_m, \tag{2}$$

following Mogi (1966) for silicate rocks, where J_m is the maximum shear stress and P_m is the mean pressure.

P.—19

Table 1. Average physical properties of the shale and sandstone rocks used for calculations.

Property	Shale	Sandstone
Density (ρ_0)	2·45 g/cm^3	2·10 g/cm^3
Porosity (ϕ^*)	12%	25%
Water content	0·04	0·02
Unconfined compressive strength (bar)	256	60
Tensile strength (bar)	30	19
Ultrasonic pulse velocity (km/sec)	2–2·95	1·4–2·7
Young's modulus (kg/cm^2)	0·8 × 10^5	0·5 × 10^5
Poisson's ratio	0·10	0·28

* $\phi = (\rho_G - \rho_0)/\rho_G$, where ρ_G is the grain density and ρ_0 is the bulk density of the rock.

The average physical and mechanical properties of shale and sandstone rocks, used in the calculation, are given in table 1.

4. Calculations and results

The total energy of the device, 12 kt (= 5·04 × 10^{20} ergs), was released in less than one microsecond into the device material. The resulting temperature and pressure were estimated, following Teller *et al* (1968), to be ~ 4 million degrees K and ~ 70 Mbar respectively. At this temperature, the device materials would have got completely vaporized. This gas then expanded rapidly and adiabatically to fill the emplacement chamber.

4.1 *Shock vaporisation and shock melting*

To determine the shock-vaporised and shock-melted regions of rock, a fine mesh calculation was done. The energy of the device ($W = 12$ kt) was distributed uniformly as internal energy of sphere of 'iron gas', whose volume is equal to that of the emplacement chamber. The vaporisation phase was found to be completed at about 150 μsec and the total mass of the rock vaporised was 640 tons which extends up to a radius of 4·1 m from the shot point. About 2000 tons of the rock, extending upto a radial distance of 6·2 m, was shock melted in about 600 μsec. The amounts of rock shock vaporised and shock-melted are 53 tons/kt and 160 tons/kt respectively, which are lower than the values of 70 tons/kt and 300 tons/kt respectively calculated for USA hard rock events (Butkovich 1967).

4.2 *Shock propagation and cavity growth*

These calculations were performed using the so-called 'bubble model' (Butkovich 1967). The total energy of 12 kt was redistributed uniformly in the spherical mass of
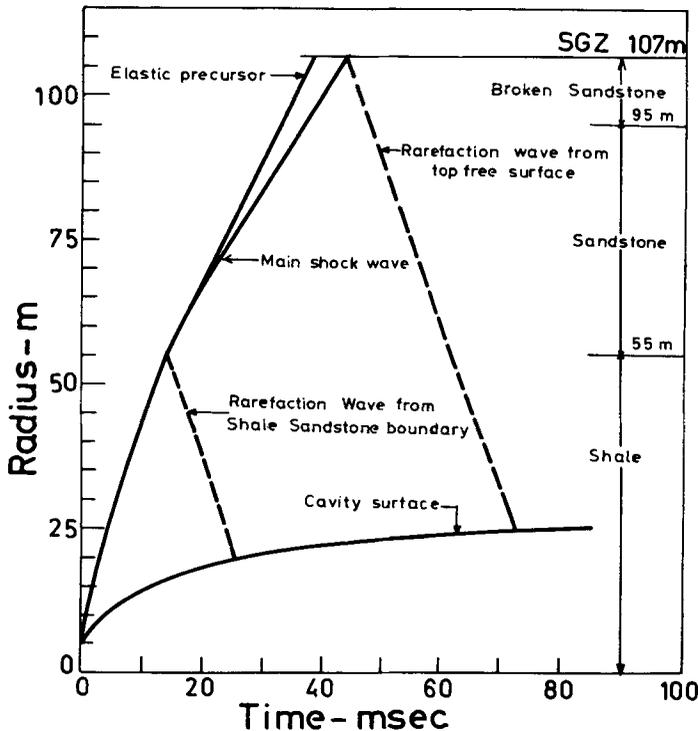
Figure 5. Computed wave propagation and cavity growth in vertical direction for Pokaran experiment.

vaporised rock of radius 4·1 m. At this energy density, the spherical cavity had uniform pressure of about 1·6 megabars. The equation of state used for the vaporised rock was the one for a 'SiO$_2$ + 1 % H$_2$O' gas mixture taken from Butkovich (1967).

The position of the first shock, the rarefaction wave and the cavity growth are plotted in figure 5. The shock position was taken to be the point where the magnitude of the artificial viscosity term was greatest. At about 14 msec the shock wave reached the shale-sandstone interface. At this interface a shock wave was induced in the sandstone layer while a backward moving rarefaction wave travelled in the shale medium*. The shock wave in sandstone split at about 62 m from shot point into two waves: a main shock wave and a preceeding elastic precursor which moved with the sound velocity in the medium. It can be seen that the main shock reached the free ground surface at time $t_s \simeq 41$ msec and got reflected from there as a rarefaction wave and met the top of the growing cavity at $t_g = 72$ msec.

The radius of the cavity at time t_g, in the vertical direction was 24·5 m compared to 23·5 m in a horizontal direction (all-shale calculation). This difference is caused by the rarefaction wave produced by the reflection of the first shock at the shale-sandstone interface. As upto time t_g (Rodinov et al 1971) the cavity radius is able to attain 80–90 %

---

* From this time onwards, the one dimensional symmetry of the problem is lost and the calculations using 'OCENER' are strictly valid for the vertical direction connecting the shot point and the surface ground zero.

of its final value, the final cavity radius in horizontal direction is estimated to be 28–29·5 m. This is in comparison with post-shot measured value of 30 m.

4.3 *Particle velocity profiles*

The particle velocity versus time at distances 27·4 m, 55 m, 80·5 m and 107 m from the shot points are plotted in figure 6. The first outward going shock wave (indicated by the sharp increase in the particle velocity) appears at these distances around 6·4, 16, 29 and 41 msec respectively. Surface ground zero begins to move up with initial velocity of 30 m/sec. This is in good agreement with the observed velocity (25–30 m/sec).

The rarefaction wave starts from the surface ground zero and moves towards the cavity increasing the particle velocities (indicated by points A in figure 6). The plot shows that the shale-sandstone interface spalled at around 58 msec. A recompaction wave, which resulted in further increase in particle velocities (denoted by points B), seems to be arrested at the shale-sandstone boundary. This would have reached the surface at much later times and its effect on increasing the particle velocities (and hence
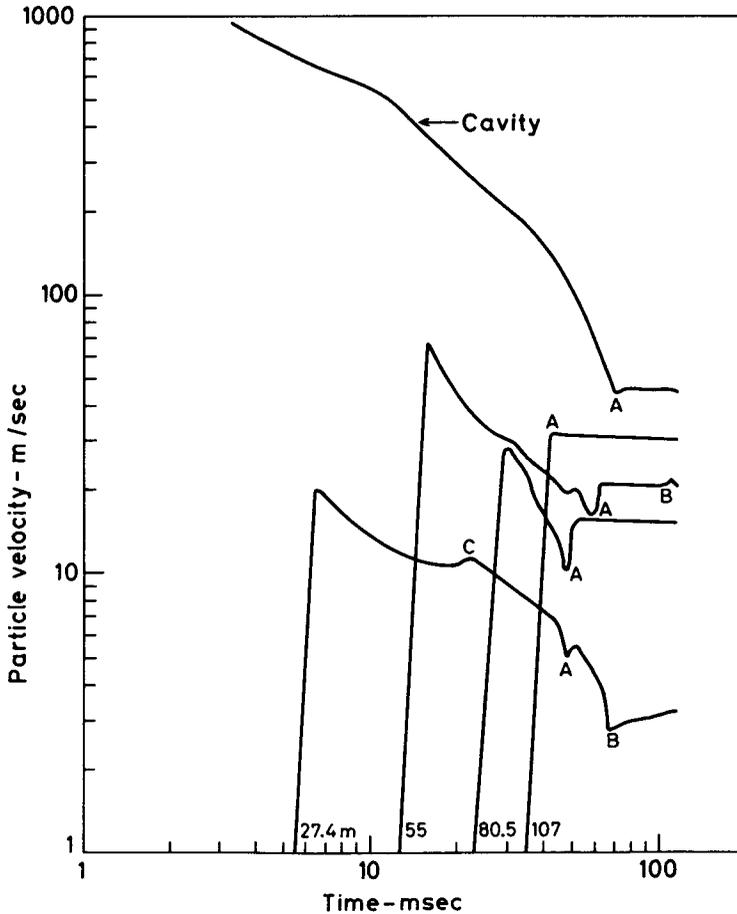

Figure 6. Computed particle velocity versus time profiles at various distances for the Pokaran PNE experiment. A — spall phase, B — gas acceleration phase.

on the final crater dimensions) would seem minimal. *This calculation seems to suggest that the principal mechanism responsible for crater formation at Pokaran was spall.*

4.4 *Extent of rock failures (ductile flow and brittle fracture)*

The calculation shows that all the rock above the detonation point (*i.e.* in vertical direction) had failed. In horizontal direction the extent of fracturing was determined by performing a calculation in homogeneous shale medium in which the free surface had been removed far away from detonation point. The maximum extent of fracture radius, as indicated by the crack number equal to 2, is about 114 m compared to the observed value of 80–100 m.

4.5 *Reasons for smaller crater in Pokaran experiment*

Having described the early time phenomenology of the Pokaran experiment, we shall in this section examine the causes for obtaining a smaller crater compared to the cratering events in hard rocks in USA. For this we will use the kinetic energy criteria as given in Appendix A.

4.5a Comparative study of cratering in Pokaran medium and Buckboard-basalt*—First, to get a preliminary idea about the cratering efficiency of the Pokaran rocks, we compare in table 2 their physical properties with those of Buckboard basalt in which USA has carried out two cratering-type nuclear explosions: Danny Boy (yield = 0·42 kt) and Sulky (0·087 kt). The USA scaled apparent crater radius and scaled apparent crater depth versus scaled depth of burst curves are essentially based on these experiments. The influence of the variation of rock properties on the cratering efficiency of a rock has been discussed by Terhune *et al* (1971) and Gupta *et al* (1979b). Based on that, we have included a comment about the relative cratering efficiency of Pokaran rocks with respect to basalt. We observe that except for the water content the other properties will lead to lowering the cratering efficiency of Pokaran rocks.

Table 2. Comparison of physical properties of Pokaran rocks with those of Buckboard-basalt.

Property	Shale	Sandstone	Basalt	Resultant cratering efficiency of Pokaran rocks relative to basalt
Density (g/cm^3)	2·45	2·10	2·62	Lower
Porosity (%)	12	25	3	Lower
Bulk modulus (kbar)	62	52	90	Lower
Water content	0·04	0·02	0·0	Higher
Maximum shear strength (bar)	358	170	300	Lower

---

* The physical properties for Buckboard-basalt have been taken from Cherry (1967).
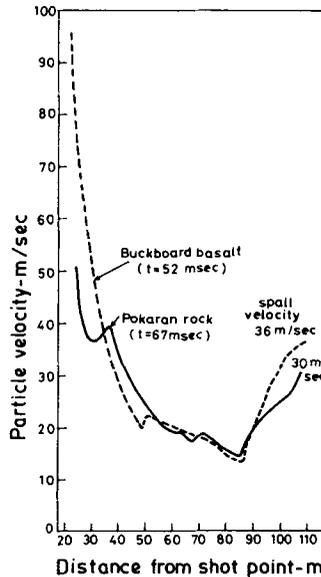
Figure 7. Particle velocity versus range profiles for the Pokaran event and a hypothetical event in Buckboard-basalt medium.

For a quantitative comparison we performed a calculation for a hypothetical event in which a device of 12 kt yield is detonated at 107 m in Buckboard basalt medium. Figure 7 shows the particle velocity versus range profile at time t_g for Pokaran event and the event in Buckboard basalt. In general the particle velocities in Pokaran medium are lower than those in Buckboard basalt. The spall velocity, as expected, is also lower (30 m/sec compared to 36 m/sec). Accordingly the cratering efficiency of Pokaran rock should be lower. This is also indicated by the values of the late-time kinetic energies along the vertical direction. These are 5·7% and 9% respectively in the two cases. Following Burton *et al* (1975), this gives us an effective equivalent yield of 5·7/9 × 12 = 7·6 kt for a detonation at 107 m in Buckboard basalt, which would give similar crater dimensions as the Pokaran experiment. Actually this may be slightly a lower estimate of the effective yield as for other than vertical directions the shock wave will traverse more through the shale medium which, as an all shale calculation shows will have more kinetic energy imparted to it. For all shale calculations, the kinetic energy at time t_g is 6·7% with corresponding effective yield of 8·9 kt. Further, there will be the effect due to interaction of shock waves at the interface of the shale-sandstone medium, which will redirect the particle velocity vectors from their initial radial directions. This is not accounted for in one-dimensional calculations. A rough estimate of this puts the effective SDOB of Pokaran experiment to be 57 m/kt$^{1/3\cdot4}$.

Considering all the above factors, we may say that the Pokaran experiment was equivalent to that of an ∼ 8 kt detonation at the same depth (effective scaled depth of burst = 58 m/kt$^{1/3\cdot4}$) in basalt. It is known that at this range of scaled depth of burial one gets a retarc or a marginal crater depending upon the bulking properties of the mound fall-back material. Since the mound in Pokaran experiment did not break and

also the post-shot analysis showed that no significant bulking of the rock had taken place, the formation of a marginal crater is not surprising.

In conclusion, the reason for obtaining a smaller crater at Pokaran is due to the fact that a smaller amount of the device energy was converted by the medium into kinetic energy. This is principally due to the geological properties of the Pokaran medium.

4.6 *Non-venting of Pokaran experiment*

According to the published radioactive vent-fraction f_c versus scaled depth of burial curve (Lapage 1974; Siddons 1974), for the Pokaran experiment at SDOB of $51.5 \text{ m}/(\text{kt})^{1/3.4}$, f_c is predicted to be very small but to have a finite value of 0·003, instead of the observed value of zero. We feel that this small discrepancy is because such scaling laws ignore the fact that the vent fraction depends not only on SDOB but also on the type of the rock medium in which the experiment is carried out. Now, as discussed above, the physico-mechanical properties of a rock reflect themselves well in the amount of energy of the explosion imparted to the rock as kinetic energy and the effective yield of an explosion relative to a standard rock medium can be defined as

$$W_1 = xW, \tag{3}$$

where x is the ratio of the kinetic energies given to rock medium and a standard rock medium by explosions of yield W carried out at the same depth of burst d. This allows us to simply modify the scaling law for f_c from

$$f_c = f(d/(W)^{1/3.4}), \tag{4}$$

to

$$f_c = f(d/(xW)^{1/3.4}), \tag{5}$$

we take

$$x = v_1^2/v^2, \tag{6}$$

where v_1 and v are the peak velocities of surface ground zero for the two explosions in a given medium and the standard medium. For quantitative estimates, we have again chosen buckboard Mesa basalt rock in USA as standard. The variation of v with d for this rock type (see Harlan 1967) is

$$v = 19700 \, (d/W^{1/3})^{-1.6}. \tag{7}$$

Here W is in kilotons and d is in meters. For Pokaran event, x turns out to be 0·5 compared to 1·0 for basalt. Using this, f_c predicted for Pokaran event is $< 10^{-6} \simeq$ zero in agreement with experiment.

To summarize, the non-venting of the Pokaran experiment seems to have been due to the smaller cratering efficiency of the shale-sandstone medium. Because only a small kinetic energy was imparted to the mound, it did not rise very high relative to the depth of burial. Consequently, the tensile stresses developed in the mound were not enough to disintegrate it and cause dynamic venting. Also, because the mound did not rise much, the minimum thickness of the overburden layer above the cavity was much larger ($\sim 24 \text{ m}$ compared to 2 m for the Danny Boy event which vented with $f_c = 0.042$) so that there was no connection of fissures. This prevented the radioactivity from leaking into the atmosphere.

Appendix A. On the correlation between the crater dimensions and the mound kinetic energy for peaceful underground explosions

The terminal effect of an underground peaceful nuclear explosion on a geological medium is to produce a crater if the depth of the burial of the explosive device is less than about $60\,\text{m/kt}^{1/3 \cdot 4*}$ (Teller *et al* 1968). The dimensions of such a crater, as indicated by many computer code calculations (Terhune *et al* 1970; Burton *et al* 1975), depend on the motion of the mound which in turn depends on the fraction of total energy of the explosive converted into the kinetic energy of the mound. Any change in the explosion conditions such as the type of the explosive, chemical or nuclear, variation in the rock properties, such as moisture content, compressibility, strength etc or geological variations such as layering, will get reflected in the amount of energy transferred to the mound and affect the crater dimensions. Although the dependence on the kinetic energy was recognised quite some time ago, no quantitative relation appears to have been deduced between it and crater dimensions. Here we attempt to show that such a relation exists.

To drive the relationship, we have carried out a similarity analysis of the linear crater dimensions versus kinetic energy of the mound following the procedure given by Baker *et al* (1973). A linear crater dimension l (l = apparent crater radius R_a or apparent crater depth D_a) produced by an explosion, beneath the surface of earth is at least a function of the explosive yield (W) and depth of burst (d). We assume that the effect of the additional variables like the type of explosive source (chemical or nuclear) and geological medium (compressibility, porosity, strength, water content, etc) is reflected in the kinetic energy (E) developed in the mound. This, we represent by a function

$$l = l(d, W, E). \tag{A1}$$

It is then easy to show from dimensional analysis that

$$l/d = f(E/W). \tag{A2}$$

This relation means that if for two craters,

$$E_1/W_1 = E_2/W_2. \tag{A3}$$

Then

$$l_1/d_1 = l_2/d_2, \tag{A4}$$

i.e. the two craters will be similar.

Though this analysis gives the functional dependence of the linear crater dimensions on the kinetic energy, the form of the function is yet undetermined. In figures A1 and A2, we have plotted R_a/d versus E/W and D_a/d versus E/W respectively for chemical explosions in Beerpaw shale. The data, which have been taken from Burton *et al* (1975), include the values of the quantities R_a and D_a and kinetic energy E, which has been calculated using computer code TENSOR (Maenchen and Sack 1964). Although there are only four points in the plots, the correlation between R_a/d and E/W and between D_a/d and E/W are clearly brought out by this data. A linear relationship is implied. It may be noted that the kinetic energy of the mound is not an observable quantity and also is not easily computable as it requires two-dimensional codes like TENSOR (Maenchen and

---

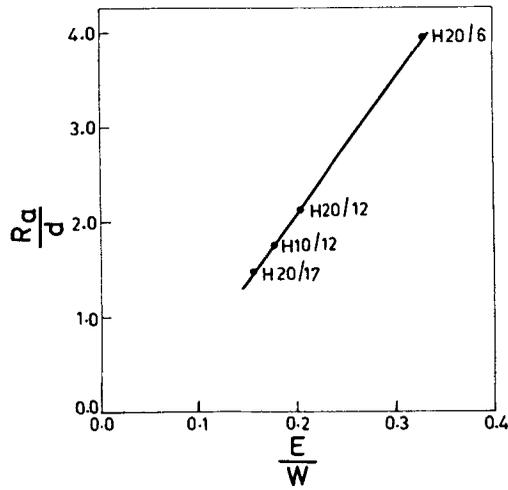* This value depends upon the geological medium.

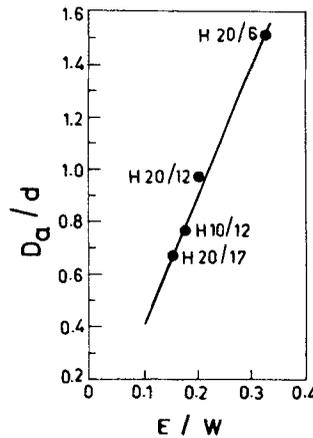**Figure A-1.** R_a/d versus E/W for Beerpaw shale.

Figure A-2. D_a/d versus E/W for Beerpaw shale.

Sack 1964). Hence for practical utilization of a crater dimension versus E/W correlation, we have to have a suitable measure for this kinetic energy. Briefly, the various equivalent measures adopted for this mound kinetic energy, as summarized by Gupta *et al* (1979b) are:

(1) velocity profile between the cavity and the free ground surface in the vertical direction at the time the rarefaction arrives at the cavity surface;

(2) free-field kinetic energy versus time profile from a calculation in which the free ground surface is not included in the calculation; and

(3) peak pressure versus radius profile.

References

Baker W E, Westine P S and Dodge F T 1973 *Similarity methods in engineering dynamics* (New Jersey: Spartan Books, Haydon Book Co.)

Burton D E, Snell C M and Bryan J B 1975 *Nucl. Technol.* **26** 65

Butkovich T R 1967 Lawrence Livermore Laboratory, Livermore Rept. UCRL-14729

Butkovich T R 1973 Lawrence Livermore Laboratory, Livermore Rept. UCRL-51441

Cherry J T 1967 *Int. J. Rock. Mech. Min. Sci.* **4** 1

Cherry J T and Petersen F L 1970 *Proc.Tech. Committee on Peaceful Nucl. Explosions I* (Vienna: IAEA) p. 241

Chidambaram R and Ramanna R 1975 *Proc. Tech. Committee on Peaceful Nucl. Explosions IV* (Vienna: IAEA) p. 421

Gupta S C and Sikka S K 1978 BARC Rept. BARC-968

Gupta S C 1979 Ph.D Thesis, Bombay University

Gupta S C, Sikka S K and Chidambaram R 1979a BARC Rept. BARC-1023

Gupta S C, Sikka S K and Chidambaram R 1979b Proc. Indian Acad. Sci. (*Earth Planet. Sci.*) **A88** 77

Harlan R W 1967 Project Pre-GONDOLA I Final Report, PNE-1107

Hearst J R 1971 Lawrence Livermore Laboratory, Livermore Rept. UCID-15783

Lapage R 1974 AWRE Rept. 011/74

Michaud L and Maury J 1970 *Proc.Tech. Committee on Peaceful Nucl. Explosions I* (Vienna: IAEA) p. 139

Maenchen G and Sack S 1964 *Methods in computational Physics* (ed.) B Adler (New York: Academic Press) **3** 181

Mogi K 1966 *Bull. Earthquake Res. India* **44** 215

Norydyke M D 1970 *Proc. Tech. Committee on Peaceful Nucl. Explosions I* (Vienna: IAEA) p. 49

Redinov V N, Aduskin V V, Kostyuchenko V N, Nikolaeusku V N, Romashov A N and Tavetkov V N 1971 Lawrence Livermore Laboratory, Livermore Report, UCRL-Trans-10671

Schatz J F 1973 Lawrence Livermore Laboratory, Livermore Rept. UCRL-51352

Siddons R A 1974 *Proc. Tech. Committee on Peaceful Nucl. Explosions III* (Vienna: IAEA) p. 353

Stephens D R, Lilley E M and Louis H 1969 Lawrence Livermore Laboratory, Livermore Rept., UCRL-71238

Teller E, Talley W K, Higgins G H and Johnson C W 1968 *The constructive uses of nuclear explosives* (New York: McGraw-Hill)

Terhune R W, Stubb T F and Cherry J T 1970 *Proc.Tech. Committee on Peaceful Nucl. Explosions I* (Vienna: IAEA) p. 415

Terhune R W 1973 Lawrence Livermore Laboratory, Livermore Rept. UCRL-91377

Toman J 1970 *Proc. Tech. Committee on Peaceful Nucl. Explosions I* (Vienna: IAEA) p. 345

Von Neumann J and Richtmayer R D 1950 *J. Appl. Phys.* **21** 232